Pergamon

Int. J. Heat Mass Transfer. Vol. 38, No. 5, pp. 843–851, 1995

0017–9310/95 $9.50+0.00

0017–9310(94)00203–7

Confined single- and multiple-jet impingement heat transfer—II. Turbulent two-phase flow

C. T. CHANG,† G. KOJASOY‡ and F. LANDIS

Department of Mechanical Engineering, University of Wisconsin–Milwaukee, Milwaukee, WI 53201, U.S.A.

and

S. DOWNING

4747 Harrison Avenue, Sundstrand Corporation, Rockford, IL 61125, U.S.A.

(*Received* 8 *November* 1993 *and in final form* 1 *July* 1994)

Abstract—The single-phase confined and submerged jet impingement heat transfer studies presented in Part I are here extended to two-phase flows with Freon R-113. Correlations are developed showing the influence on heat transfer of jet Reynolds number, flow quality, plate spacings and, for multiple jets, pitch-to-jet diameter ratio. In all cases the Nusselt numbers obtained are referenced back to single-jet, single-phase conditions. It is shown that the heat transfer rate can be improved significantly over that possible with a single-phase liquid operating with the same geometry although, depending on the configuration, the pressure drop encountered with two-phase cooling may not be acceptable.

1. INTRODUCTION AND BACKGROUND FROM LITERATURE

Increased cooling demands in electronic modules have led to investigations of two-phase jet impingement subcooled boiling as a possible answer to higher heat loads. Much of the literature deals with the critical heat flux for single free jets, i.e. boiling caused by impinging liquid jets flowing through ambient air. Work with submerged jets, where the impinging liquid is the same as the surrounding fluid, was done by Ma and Bergles [1]. Multi-jet two-phase impingement cooling was studied by Sakhuja *et al.* [2], while bubbly flow impinging on a confined wall was studied by Serizawa *et al.* [3]. More recent work emphasizing critical heat flux is due to Mudawar and Wadsworth [4] and Wadsworth and Mudawar [5].

This study was carried out to extend the single-phase fluid cooling in CHIC (compact high intensity cooler) units reported in Part I to two-phase flows where higher Nusselt numbers should be expected. Although in most applications the entering fluid will be subcooled, the successive coolant flow through multiple fins may lead to a fluid already in the two-phase regime impinging on a subsequent heated fin. Thus, the aim was to correlate subcooled and saturated two-phase boiling flows for both single- and multiple-jets with the previous single-phase impingement results obtained in the same test geometries.

†Presently address: Yuen-Ze Institute of Technology, Taiwan.

‡Author to whom correspondence should be addressed.

2. EXPERIMENTAL SETUP

Most of the experimental setup has already been described in Part I. Two-phase flow in the test section was achieved by flashing slightly subcooled R-113 through adiabatic throttle valves just upstream of the test section. Assuming negligible kinetic energies, the specific enthalpy of the liquid ahead of the throttle valve equaled that of the downstream liquid–vapor mixture. Thus, the known upstream pressure and temperature permitted determination of the downstream quality when either downstream pressure or temperature were observed. Both were measured, resulting in excellent agreement. In the present tests, the inlet quality obtainable ranged up to 31% for single-jet flows, up to 23% for multiple jets.

After leaving the flashing valves, the jet experienced further pressure drop and quality increase while it passed through the jet nozzles. An energy balance, adding the heat supplied through the test section by the electric heaters, then led to the correct post-boiling fluid enthalpy. In the two-phase regime, the measured pressure and temperature in the confined region between the "nozzle" and "target" plates (see Fig. 3 of Part I for identification) were assumed to be uniform. The experimental complexity and cost of the pressurized system did not allow for critical heat flux tests.

The geometric requirement for the multi-jet tests, where the spent fluid had to vent through the target plate, limited the choice of heater to a thin foil unit. In nucleate boiling, the use of such AC heaters might lead to temperature variations that amplify the

NOMENCLATURE

(Only symbols not defined in Part I are listed here.)

c_p	specific heat at constant pressure [J kg^{-1} K^{-1}]
g	acceleration due to gravity [m s^{-2}]
h_{fg}	enthalpy of evaporation [J kg^{-1}]
j	mixture volumetric flux [m^3 s^{-1}]
j_f	superficial velocity or volumetric flux of liquid phase [m s^{-1}]
m	exponent in equation (8)
$\dot{m}$	mass flow rate [kg s^{-1}]
$\overline{Nu}$	Nusselt number
$\overline{Nu}(R)$	cell average Nusselt number
$\dot{q}$	heat transfer rate [W]
Re	Reynolds number
x	quality.

Greek symbols

Δ	difference
ν	kinematic viscosity [m^2 s^{-1}]
ρ	density [kg m^{-3}]
σ	surface tension [N m^{-1}]
χ_{tt}	turbulent two-phase flow Martinelli parameter, defined by equation (18).

Subscripts

CSP	convective single-phase
CTP	convective two-phase
f	liquid phase
fg	transition from liquid to vapor phase
fo	refers to total two-phase mixture flow velocity as if it was a saturated liquid only
g	gas or vapor only
j	jet or jet (orifice) diameter
m	two-phase mixture
pre	predicted, based on applicable correlation
sat	saturation temperature
SCB	subcooled boiling
SNB	saturated nucleate boiling
sub	subcooling
TP	two-phase flow.

Superscripts

$\cdot$	refers to per unit time
$-$	refers to average value from $r = 0$ to $r = r$
$''$	refers to per unit area.

inherent flow fluctuations although the effect is likely to be small in the highly turbulent flow existing in multi-jet cooling.

3. BOILING MODEL

It is widely accepted that two types of behavior occur in convective boiling:

(a) In nucleate boiling, bubbles are formed by nucleation at a solid surface. In saturated boiling, these bubbles grow, detach and join the main two-phase flow. In highly subcooled boiling, they collapse rapidly while heating the main liquid flow towards the saturation temperature. In slightly subcooled boiling, the behavior resembles that of saturated boiling, although bubbles still recondense in the main stream. In all cases, the heat transfer due to nucleate boiling is increased by the degree of wall superheat.

(b) In convective boiling heat is transferred by conduction and convection through a thin liquid film with the amount substantially increased by bubble dynamics. Thus, any procedure for calculating flow boiling must have elements of both nucleate and convective boiling. Rohsenow [6] first suggested that flow boiling be viewed as an additive process, combining nucleate pool boiling with the forced flow heat transfer while assuming the two mechanisms to be independent. This approach has since been improved by Chen [7] who introduced weighing functions to allow for interaction between the two mechanisms.

The superposition method was found to be most effective with the assumption that both the nucleate and the convective mechanisms occur over the entire range of flow conditions. Thus, on a per unit area basis

$$\dot{q}''_{TP}(r) = \dot{q}''_{CTP}(r) + \dot{q}''_{SNB}(r) \quad (1)$$

where $\dot{q}''_{TP}(r)$ is the local total heat flux, $\dot{q}''_{CTP}(r)$ is the contribution due to the two-phase convection, $\dot{q}''_{SNB}(r)$ is due to nucleate boiling, and r is the radial distance from the stagnation point. Alternatively, in terms of heat transfer coefficients,

$$\dot{q}''_{CTP}(r) = h_{CTP}(r)[T_w(r) - T_b(r)] + h_{SNB}(r)[T_w(r) - T_b(r)]. \quad (2)$$

Here h_{CTP} and h_{SNB} are defined as the local heat transfer coefficients due to two-phase convection and nucleate boiling, respectively, while T_w and T_b are the local wall and bulk-fluid temperatures, respectively.

With saturated boiling T_{sat} replaces T_b to yield

$$\dot{q}''_{TP}(r) = h_{CTP}(r)\Delta T_{sat} + h_{SNB}(r)\Delta T_{sat} \quad (3)$$

where ΔT_{sat} is the degree of wall superheat ($T_w - T_{sat}$). The total heat transfer coefficient for saturated boiling then becomes

$$h_{TP}(r) = h_{CTP}(r) + h_{SNB}(r). \quad (4)$$

The nucleate boiling component can be determined by experiments with subcooled pool boiling. Once it is known, the convective contribution is determined from equation (1) by subtracting the nucleate portion from the total measured heat flux.

The superposition specified by equation (1) is also assumed to hold throughout the subcooled boiling range, including the partially subcooled and fully-developed subcooled boiling regions. The total heat flux then becomes

$$\dot{q}''_{TP}(r) = \dot{q}''_{CSP}(r) + \dot{q}''_{SCB}(r) \quad (5)$$

where $\dot{q}''_{CSP}$ is defined as the convective heat flux for single-phase liquid jet-impingement, and $\dot{q}''_{SCB}$ is the subcooled boiling contribution. In terms of heat transfer coefficients, equation (5) becomes

$$\dot{q}''_{TP}(r) = h_{CSP}(r)(\Delta T_{sub} + \Delta T_{sat}) + h_{SCP}(r)\Delta T_{sat}(r) \quad (6)$$

where $\Delta T_{sub} \equiv T_{sat} - T_b$ is the degree of subcooling.

Here $h_{CSP}(r)$ is considered to be known from single-phase jet-impingement experiments as shown in Part I. From a series of subcooled boiling jet-impingement experiments, the subcooled boiling contribution is evaluated from

$$\dot{q}''_{SCB}(r) = \dot{q}''_{TP}(r) - \dot{q}''_{CSP}(r). \quad (7)$$

The heat flux in fully-developed subcooled boiling has been shown by many workers to be

$$\dot{q}''_{SCB} = A(\Delta T_{sat})^m \quad (8)$$

with m typically from 3.0 to 4.0. In terms of a heat transfer coefficient equation (8) becomes

$$h_{SCB} = A(\Delta T_{sat})^{m-1} \quad (9)$$

where A is a parameter characterizing the fluid–solid surface combination and fluid properties. According to ref. [6], it is given by

$$A \equiv \left[\frac{\mu_f h_{fg}}{(\sigma/g\Delta\rho)^{1/2}}\right]\left(\frac{c_{pf}}{C_{fs} h_{fg} Pr_f^{n+1}}\right)^m. \quad (10)$$

Here all the variables, except for the surface–fluid parameter, C_{fs}, are known once n is set as 0.7 as suggested by Rohsenow.

The approach outlined above will hold in partial subcooled boiling as well as in fully-developed subcooled boiling. However, as fully-developed subcooled boiling is approached, the subcooled boiling contribution gradually overshadows the single-phase liquid convection contribution. In a log–log plot of $\dot{q}'' = f(\Delta T_{sat})$, this fully developed region appears as a straight line, allowing for the determination of the exponent m in equations (8)–(10).

4. DATA REDUCTION FOR SINGLE-JET IMPINGEMENT

4.1. *Subcooled boiling experiments*

Typical experimental single-jet stagnation point data for subcooled boiling are plotted in Fig. 1 in terms of heat flux vs ΔT_{sat} at an essentially fixed jet velocity for different initial levels of subcooling. Similar results are obtained at fixed subcooling for different jet velocities. Matching the results of others, with increasing heat flux all data points approach the same limiting straight line on a log–log plot in fully-developed subcooled boiling (shown here as a solid line), irrespective of initial subcooling level or jet velocity. From the slope of these limiting curves and a known value of $\dot{q}''$ (at a high value of ΔT_{sat}), both A and m in equation (8) can be determined.

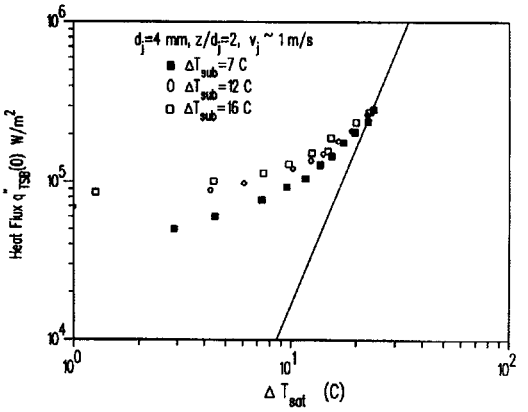

Fig. 1. Heat flux vs ΔT_{sat} for single-jet subcooled boiling stagnation point heat transfer at fixed jet velocity. Solid line is best interpolation of limiting slope.

Over the full range of test results including different initial subcooling, various values of z/d_j, and different jet velocities, the best interpolation of the average limiting slope was $m = 3.5$. The experimentally determined value of A then led to $C_{fs} = 0.0091$ for the R-113–nickel surface combination. This is well within the range of published data.

4.2. *Nucleate boiling contribution*

The nucleate boiling contribution, which will be a function of ΔT_{sat}, now becomes

$$\dot{q}''(r) = \left(\frac{\mu_f h_{fg}}{(\sigma/g\Delta\rho)^{1/2}}\right)\left(\frac{c_{pf}\Delta T_{sat}(r)}{C_{fs} h_{fg} Pr_f^{1.7}}\right)^{3.5}. \quad (11)$$

The results illustrated in Fig. 1 may also be compared to the work of Ma and Bergles [1] for unconstrained subcooled jet impingement boiling of R-113. These authors observed the same transition from partial subcooled convective flow to fully-developed subcooled boiling heat transfer. Their results also converged to a fixed slope as suggested by equation (8). However, while the present tests led to $m \simeq 3.5$ with ΔT_{sat} of about 15°C at a heat flux of 10^5 W m^{-2}, at different pressure levels and surface conditions Ma and Bergles found $\Delta T_{sat} \approx 20$–23°C at that heat flux and m at the exceptionally high value of about 5–6.

In line with the procedure outlined in Part I, the radial temperature distribution was again determined by fitting a fourth-order least square polynomial

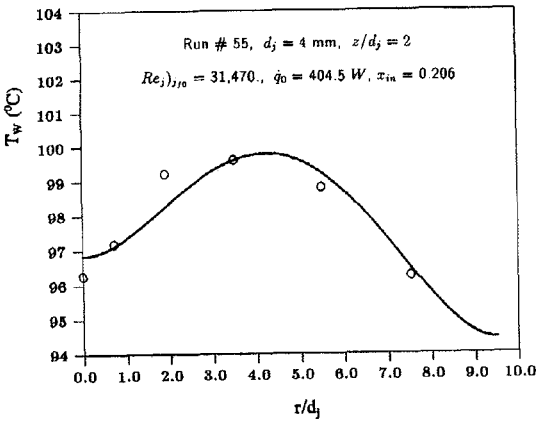

Fig. 2. Curve fit of target plate surface temperatures for high heat transfer rate, single-jet, two-phase flow with high inlet quality.

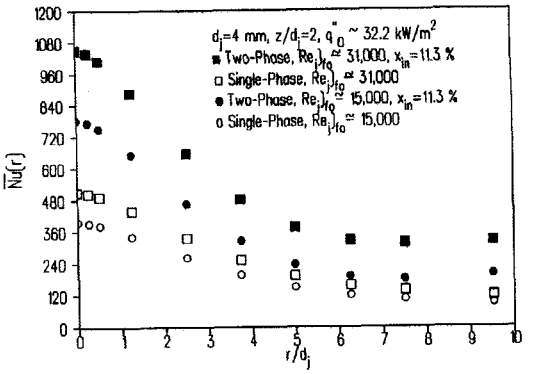

Fig. 3. Comparisons of local average Nusselt numbers vs radial distance from stagnation point for single-jet, single- and two-phase flows at various Reynolds numbers (values are computed, not experimental, values at points shown).

through the temperature data measured at six radial locations. Typical results are illustrated in Fig. 2 for a high heat flux case with an inlet quality of about 20%. Here the Reynolds number is defined by

$$Re_{j_{fo}} \equiv \frac{\rho_f j_{fo} d_j}{\mu_f} \tag{12}$$

where ρ_f and μ_f are the density and viscosity of the saturated liquid, while j_{fo} is the volumetric flux of the mixture assuming the total mixture to be at the saturated liquid state. In this definition, the Reynolds number will not change if the quality is increased at a given mass flow rate. However, the increase in mixture mean velocity with increasing quality (at constant mass flow rate) should lead to both higher turbulence and heat transfer. Thus the effect of quality still has to be accounted for separately.

Allowing for the correct local bulk fluid temperature, $T_b(r)$, the local heat transfer coefficient can then be defined by

$$h_{TP}(r) \equiv \dot{q}''_{TP}(r)/[T_w(r) - T_b(r)]. \tag{13}$$

For subcooled boiling, the local bulk fluid temperature was calculated via an energy balance from the nozzle jet exit to the local radial condition. It was taken as $T_b(r) = T_{sat}$ for saturated boiling.

Again, the results are presented in terms of the local average heat transfer coefficient, $\bar{h}$, or the local average Nusselt number, $\overline{Nu}$, defined by

$$\bar{h}(r) \equiv \overline{\dot{q}''}(r)/[\overline{T_w}(r) - T_b(r)]; \quad \overline{Nu}(r) \equiv \bar{h}(r) d_j/k_f. \tag{14}$$

Here local average values are calculated as area averages by

$$\overline{\dot{q}''}(r) \equiv \left(\frac{2}{r^2}\right)\int_0^r \dot{q}''(r) r\,dr; \quad \overline{T(r)} \equiv \left(\frac{2}{r^2}\right)\int_0^r T(r) r\,dr. \tag{15}$$

The local average Nusselt number is not only more useful than the local Nusselt number for a designer of a multi-jet impingement cooler, it will also be more accurate since the influence of local temperature errors will be reduced by the least square fit. Such possible errors tended to be highest for low heat loads and high inlet qualities where the radial temperature variation along the impingement plate remained small. Thus most credence should be given to those experimental results where the inlet quality is low and the heat flux high, leading to moderately high radial temperature gradients. Fortunately, these are also the conditions of greatest practical interest.

Figure 3 compares the local average Nusselt numbers computed from the fitted temperature profiles at various locations for single- and two-phase flows at the same two sets of Re_{jfo}. Two-phase flow, with its higher average velocity at the same defined Reynolds number, will lead to a higher heat transfer than the single-phase case. The apparent increase of $\overline{Nu}(r)$ at large values of r/d_j is an anomaly caused by the physical boundary conditions being different from those assumed in the analysis. Instead of having zero radial or axial heat flux near the outer radius of the heating plate, some heat loss actually did take place, although the effect was pronounced only at r/d_j values significantly beyond those encountered in practice. The tests also indicated that $\overline{Nu}(r)$ increased with higher inlet quality at the same Re_{jfo}. This may be due, at least in part, to the additional turbulence caused by the increased number of vapor bubbles, confirming the role of upstream turbulence on stagnation point heat transfer variously observed in single-phase impingement flows.

Figure 4 shows the log–log relation between ΔT_{sat} and the inlet quality at essentially constant Reynolds number. The same slope applies throughout suggesting a single applicable power law for the fit between ΔT_{sat} and inlet quality. Similarly, there is an almost constant direct power-law relation between heat flux and ΔT_{sat} at constant Reynolds number as shown in Fig. 5 with inlet quality as the parameter.

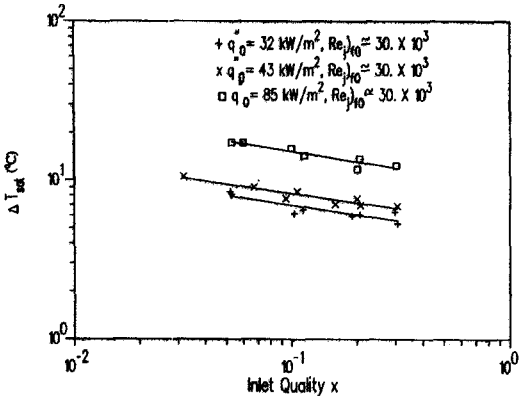

Fig. 4. ΔT_{sat} vs inlet quality for single-jet, two-phase flows at constant Reynolds number but for various heating rates. Solid lines represent best least square fit.

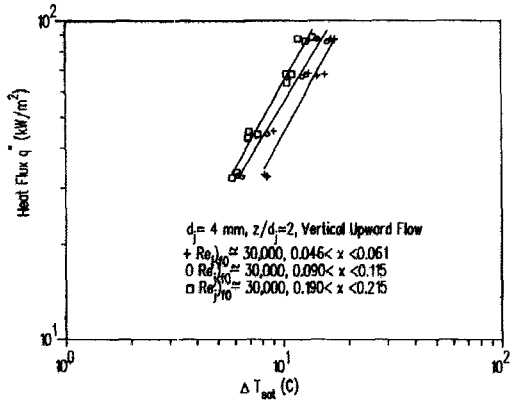

Fig. 5. Effect of heat flux vs ΔT_{sat} in single-jet, two-phase flow at constant Reynolds number and varying inlet quality. Solid lines represent best least square fit.

This suggests that inlet quality does not change the nature of the power law for heat flux vs ΔT_{sat}. However, the higher the inlet quality, the lower the wall superheat (and the higher the Nusselt number) will be for the same heat flux.

All data discussed so far were for vertical upflow. Nusselt numbers differed by less than 3.6% for horizontal or vertical downflows over the heat flux, Reynolds number and inlet quality range tested. Thus, from a design point of view, in this test range the nucleate boiling Nusselt number may be assumed to be independent of flow orientation as long as conditions are far from critical heat flux.

5. SINGLE-JET BOILING CORRELATIONS

Here the convective boiling correlations will be developed as a modified version of the single-phase flow correlation, while the nucleate boiling contribution will again be adapted from the case of subcooled boiling.

An effective Reynolds number, R_{jjf}, can be defined by

$$Re_{jjf} \equiv \frac{\rho_f j_f d_j}{\mu_f} \tag{16}$$

where the density and viscosity are based on the liquid phase while j_f is the liquid superficial or volumetric flux given by

$$j_f \equiv \frac{\dot{m}_f}{A_j \rho_f} = \frac{\dot{m}_m (1-x)}{A_j \rho_f}. \tag{17}$$

Here $\dot{m}_m$ is the mixture flow rate, $\dot{m}_f$ the liquid flow rate and A_j the nozzle exit area. Following Lockhart and Martinelli [8], the two-phase turbulent heat transfer coefficient can be correlated by the Martinelli parameter

$$\chi_{tt} = \left(\frac{1-x}{x}\right)^{0.9} \left(\frac{\rho_g}{\rho_f}\right)^{0.5} \left(\frac{\mu_f}{\mu_g}\right)^{0.1}. \tag{18}$$

Using the above definitions, the higher the inlet quality for a given mass flow rate, the lower will be the jet Reynolds number defined by equation (16). The other flow variables relating the liquid to the vapor portions are contained in χ_{tt}.

In saturated boiling the total heat transfer is again assumed to be the sum of the convective and the nucleate boiling components, both applied to ΔT_{sat}. This leads to

$$\bar{h}_{CTP}(r) = \bar{h}_{TP}(r) - \bar{h}_{SNB}(r). \tag{19}$$

The total heat flux $\bar{q}''_{TP}(r)$ was computed from the fitted temperature profile, while $\bar{q}''_{SNB}(r)$ was taken directly from the subcooled boiling correlation, equation (11).

The net difference, expressed in terms of computed Nusselt numbers, describes the portion assigned to convective boiling and is illustrated by the squares in Fig. 6(a) for the case of a low inlet Reynolds number, a low heat flux and a 6.7% inlet quality. The solid line corresponds to the correlation suggested subsequently. Corresponding typical data for a higher inlet Reynolds number, an inlet quality of 21% and a higher heat flux are shown in Fig. 6(b). The small contribution due to nucleate boiling may be noted in both figures. The increase of $\overline{Nu}(r)$ at r/d_j beyond the normal design region ($r/d_j \approx 5$) is again due to experimental radial and axial heat losses not accounted for in the model. In both figures, the solid line corresponds to the correlation suggested subsequently.

Over the actual plate spacing ($1.5 \leqslant z/d_j \leqslant 6.0$) and Reynolds number ranges, no effect of these two variables was found in the ratio of convective two-phase Nusselt number divided by single-phase Nusselt number at the stagnation point. However, results were very sensitive to inlet quality. This led to an attempted correlation, shown in Fig. 7, where, for all two-phase data, the ratio

$$\frac{\text{convective component of two-phase stagnation point heat transfer coefficient}}{\text{corresponding single-phase convection heat transfer coefficient}} - 1$$

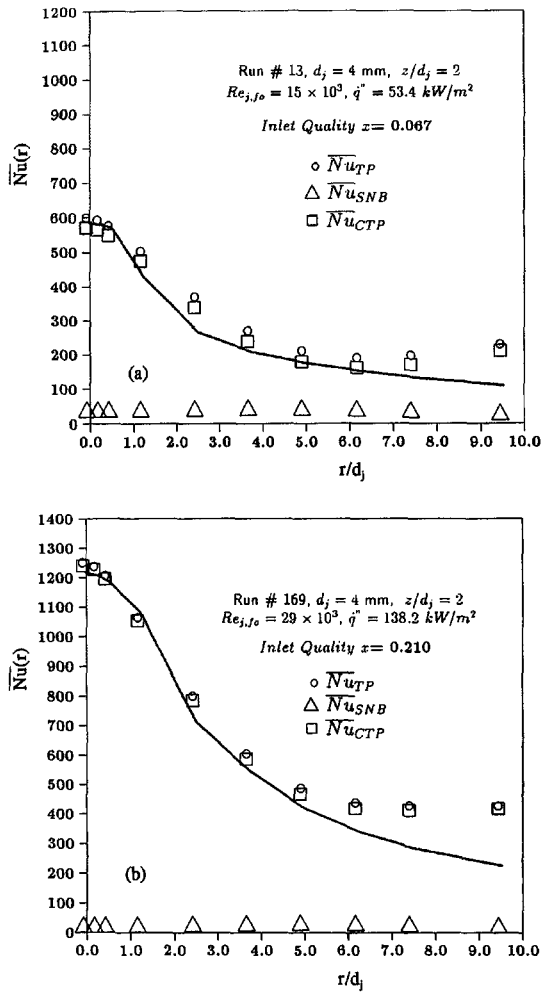

Fig. 6. Local average Nusselt number vs distance from stagnation point showing convective and nucleate boiling contributions in single-jet flow (points shown are computed rather than experimental values): (a) low Reynolds number and inlet quality case; (b) higher inlet Reynolds number and inlet quality.

is plotted against the inverse of the stagnation point Martinelli parameter, $1/\chi_{tt}$. From a log–linear least square fit of the data in Fig. 7, the stagnation point convective heat transfer coefficient component could be correlated by

$$h_{CTP}(0) = h_{CSP}(0)[1.0 + 1.187\chi_{tt}^{-0.438}(0)]. \quad (20)$$

To develop a correlation for local average Nusselt numbers as function of radius, a modified heat transfer coefficient ratio (as defined on the figure) vs the difference of the Martinelli parameters between the stagnation point value and the local radius value, denoted by $\Delta\chi_{tt}$, was plotted in Fig. 8. This suggested that the modified heat transfer coefficient ratio remains invariant up to $\Delta\chi_{tt} \approx 0.02$ while it decreases for larger values of $\Delta\chi_{tt}$. For simplicity's sake, this decrease was taken to be linear. This led finally to the convective average heat transfer coefficients for

$$\bar{h}_{CTP}(r) = \bar{h}_{CSP}(r)[1.0 + 1.187\chi_{tt}^{-0.438}(0)]\Delta\chi_{tt} \leqslant 0.02$$

$$\bar{h}_{CTP}(r) = \bar{h}_{CSP}(r)[1.0 + 0.7846\Delta\chi_{tt}^{-0.15}\chi_{tt}^{-0.438}(0)]$$

$$\Delta\chi_{tt} > 0.02.$$

Adding the nucleate boiling component, equation (11), to the convective boiling results, finally leads at the stagnation point to

$$h_{TP}(0) = \left[\frac{h_{fg}\mu_f}{(\sigma/g\Delta\rho)^{1/2}}\right]\left(\frac{c_{pf}}{C_{fs}h_{fg}Pr^{1.7}}\right)^{3.5}[\Delta T_{sat}(0)]^{2.5} + h_{CSP}(0)[1.0 + 1.187\chi_{tt}^{-0.438}(0)] \quad (23)$$

and, for $r > 0$ with $\Delta\chi_{tt} > 0.02$,

$$\bar{h}_{TP}(r) = \left[\frac{\mu_f h_{fg}}{(\sigma/g\Delta\rho)^{1/2}}\right]\left(\frac{c_{pf}}{C_{fs}h_{fg}Pr^{1.7}}\right)^{3.5}[\Delta T_{sat}(r)]^{2.5} + h_{CSP}(r)\{1 + 0.611\Delta\chi_{tt}^{-0.15}[1.187\chi_{tt}^{-0.438}(0)]\} \quad (24)$$

while, for $\Delta\chi_{tt} \leqslant 0.02$,

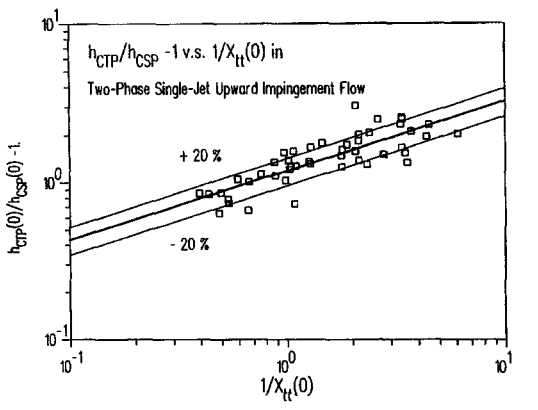

Fig. 7. Modified ratio of two-phase to single-phase stagnation point heat transfer coefficient vs inverse of Martinelli parameter for upward flow single- and two-phase tests.

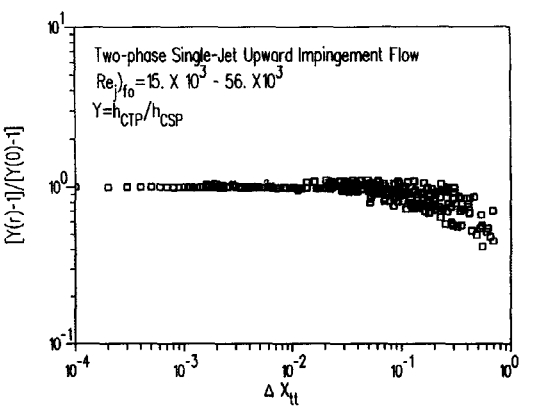

Fig. 8. Ratio of modified local average heat transfer coefficient divided by stagnation point heat transfer coefficient vs difference in Martinelli parameters for single- and two-phase flows.

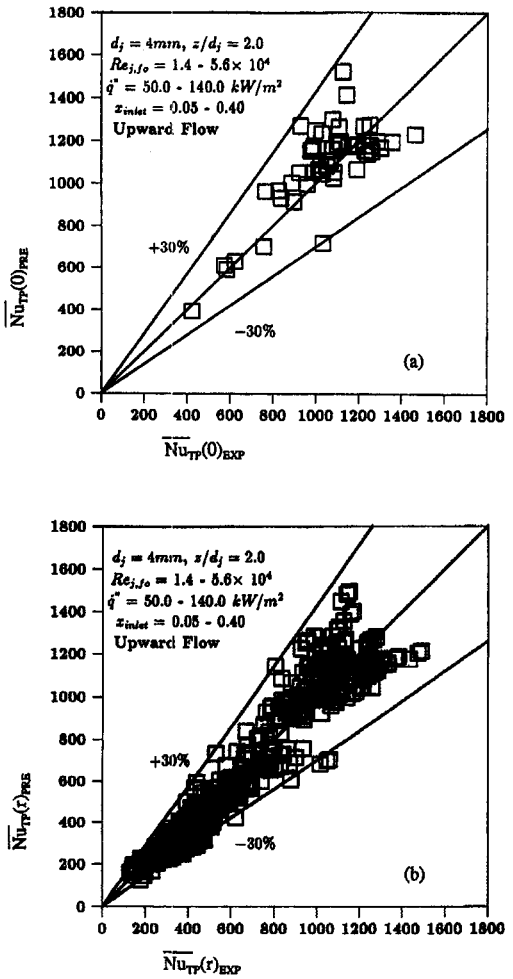

Fig. 9. Comparison of experimental Nusselt number with predictions from correlations for two-phase, single-jet flows: (a) stagnation point Nusselt number; (b) local average Nusselt number.

$$\bar{h}_{TP}(r) = \left[\frac{\mu_f h_{fg}}{(\sigma/g\Delta\rho)^{1/2}}\right]\left(\frac{c_{pf}}{C_{fs}h_{fg}\,Pr^{1.7}}\right)^{3.5}[\Delta T_{sat}(r)]^{2.5} + h_{CSP}(r)[1.0+1.187\chi_{tt}^{-0.438}(0)]. \quad (25)$$

As a final check on this correlation, Figs. 9(a) and (b) show the predicted Nusselt number vs experimental values together with ±30% deviation lines. Figure 9(a) refers to the stagnation point Nusselt number predicted from equation (23), whereas Fig. 9(b) refers to the local average Nusselt number predicted by equations (23) and (24). The correlations hold equally for vertical upflow, vertical downflow and horizontal flow.

The use of the above equations to predict the local average Nusselt number is illustrated by the solid lines in Figs. 6(a) and (b), showing reasonable agreement between experiment and correlation for the range of r/d_j of practical interest. These results are considered to be within the predictive accuracy of most two-phase flow correlations. A separate uncertainly analysis indicated that the Nusselt number accuracy should be ±40%.

6. MULTIPLE-JET TWO-PHASE IMPINGEMENT HEAT TRANSFER

In multiple-jet two-phase heat transfer, a distinction must again be made between subcooled and two-phase flow boiling. For the subcooled boiling regime, it is again assumed that the results are not sensitive to geometry. Thus the slope of the log heat flux vs log ΔT_{sat} line (here $m = 3.5$) is taken to be the same for pool boiling, forced convection flow boiling, and single- or multiple-jet impingement boiling.

What may change is the coefficient A in equation (10), reflecting both the changes in geometry and the different surface parameter C_{fs} for the inconel–R-113 interface used here instead of the nickel–R-113 interface used for the single-jet tests. However, a change in the intercept value (or the value of ΔT_{sat} where partial boiling becomes fully developed boiling), should have little impact on the final result since again, for moderate values of ΔT_{sat}, the convective heat transfer far outweighs the boiling component.

The data reduction led again to the use of a local average Nusselt number as function of the radius. For a fixed $p/d_j = 10$, the experimental data were plotted on Fig. 10(a) for $z/d_j = 3$ and Fig. 10(b) for $z/d_j = 6$ as log–log functions of $\overline{Nu}(R)$ vs Re_j together with the corresponding predictions from the single-jet two-phase flow analysis. $\overline{Nu}(R)$ indicates the local average Nusselt number over an equivalent cell area as discussed in Part I. Similar results were obtained for $p/d_j = 5$. Both data and predictions account for a range of inlet qualities. Even though the single-jet data consistently underpredict the multiple-jet results, it appears that the Reynolds number variation is essentially the same, irrespective of the p/d_j ratio. For the two sets of pitch-to-diameter ratio tested, no consistent or significant variation with p/d_j could be determined. However, it appeared that an additional z/d_j relation in the form

$$f(z/d_j) = 1.667(z/d_j)^{-0.116} \quad (26)$$

similar to the behavior already observed in Part I for multiple-jet flows of a single-phase fluid away from the stagnation point, would improve the prediction.

Incorporating this relation into the Nusselt number predictions arising from the single-jet results, equations (25) and (24), finally lead to

$$\overline{Nu}_{CTP,multi\text{-}jet}(r) = 1.667\overline{Nu}_{CSP,single\text{-}jet}(r)(z/d_j)^{-0.116} \times\left[1.0+1.187\left(\frac{1}{\chi_{tt}(0)}\right)^{0.438}\right]; \quad \text{for } \Delta\chi_{tt} \leqslant 0.02 \quad (27)$$

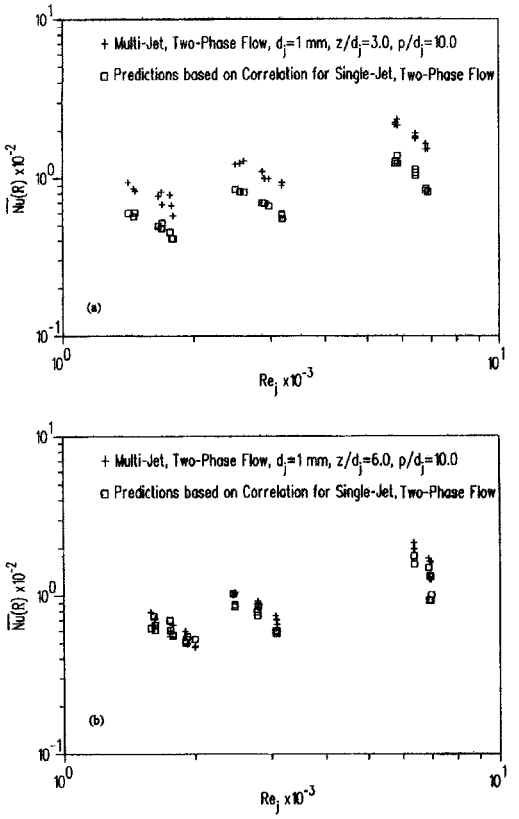

Fig. 10. Comparison of local average Nusselt numbers over a cell area for multi-jet, two-phase flow with predictions from single-jet, two-phase flow correlation: (a) $z/d_j = 3$ and (b) $z/d_j = 6$.

$$\overline{Nu}_{\text{CTP,multi-jet}}(r) = (1.667\overline{Nu}_{\text{CSP,single-jet}}(r)(z/d_j)^{-0.116}) \times \left[1.0+0.7846\Delta\chi_{tt}^{-0.15}\left(\frac{1}{\chi_{tt}(0)}\right)^{0.438}\right]$$

$$\text{for } \Delta\chi_{tt} > 0.02. \quad (28)$$

The convective portion of the heat transfer is now given by

$$\bar{q}''_{\text{CTP,multi-jet,pre.}}(r) = \frac{\overline{Nu}_{\text{CTP,multi-jet,pre.}}(r)\Delta T_{\text{sat}}(r)k_f}{d_j} \quad (29)$$

to which again the nucleate boiling component, which depends only on T_{sat}, has to be added, leading to, in terms of heat flux and Nusselt number, respectively

$$\bar{q}''_{\text{Total,multi-jet,pre.}}(r) = \bar{q}''_{\text{Total,multi-jet,pre.}}(r) + \bar{q}''_{\text{SNB}}(r) \quad (30)$$

$$\overline{Nu}_{\text{Two-phase,multi-jet,pre.}}(r) = \overline{Nu}_{\text{CTP,multi-jet,pre.}}(r) + \left(\frac{q''_{\text{SNB}}(r)}{T_w(r) - T_{\text{sat}}}\right)\left(\frac{d_j}{k_f}\right). \quad (31)$$

Although somewhat complicated, these correlations match the actual experimental data very well as shown in Fig. 11 where ±20% confidence limits are also given.

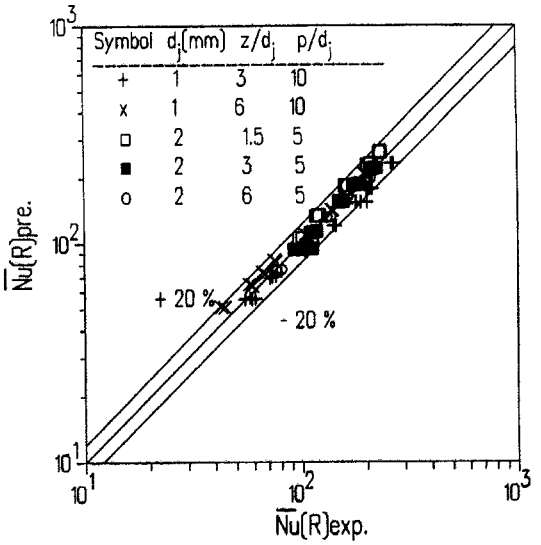

Fig. 11. Comparison of experimental local average Nusselt numbers with predictions from correlations for two-phase, multiple-jet impingement flow.

Considering the usual accuracy limitations in two-phase flows, the agreement appears to be satisfactory over the test range: $1640 \leqslant Re_{jfo} \leqslant 7200$, $0.05 \leqslant x \leqslant 0.23$, 11.0 kW m^{-2} $\leqslant$ heat flux $\leqslant$ 216 kW m^{-2}, $1.5 \leqslant z/d_j \leqslant 6.0$ and $p/d_j = 5.0, 10.0$.

In an actual application, ΔT_{sat} must, obviously, be kept low enough to avoid any likelihood of critical heat flux. At higher heat fluxes, flow orientation may play a role due to the different influence of gravity, as may the possible existence of a "dead water region" in an assembly where not all vapor bubbles are swept away by the flow.

7. UTILITY OF THE RESULTS

Although adequate correlations were obtained for both single-jet and multiple-jet impingement boiling in confined, submerged flows, the utility of these results needs to be discussed. In a companion study dealing with pressure drops encountered in multiple-jet impingement cooling, Chang [9] suggests that, in general, the pressure drops through a series of multiple impingement plates are too high to make multiple plate two-phase impingement boiling attractive in spite of the attainable high heat flux. However, if boiling occurs on only one target surface, or if in a series of sequential impingement surfaces only the last one encounters two-phase conditions, then the increased heat transfer possible with boiling deserves attention.

8. SUMMARY

Experimental correlations have been presented for confined and submerged two-phase, turbulent, single-

and multiple-jet impingement boiling, starting with subcooled or two-phase R-113. The results, which are referenced back to data and correlations obtained for single-phase flows, adequately predict local average Nusselt numbers over an extended range of inlet Reynolds numbers, inlet qualities, heat flux rates, plate spacing, and, for multiple-jet flows, pitch spacings.

REFERENCES

1. C.-F. Ma and A. E. Bergles, Jet impingement nucleate boiling, *Int. J. Heat Mass Transfer* **29,** 1095–1101 (1986).
2. R. K. Sakhuja, F. S. Lazgin and M. J. Owen, Boiling heat transfer on arrays of impinging jets, ASME Paper 80-HT-47 (1980).
3. A. Serizawa, O. Takahashi, Z. Kawara, T. Komeyama and I. Michiyoshi, Heat transfer augmentation by two-phase bubbly flow impingement jet with a confining wall, *Proceedings Ninth International Heat Transfer Conference*, Jerusalem, Vol. 4, pp. 93–98 (1990).
4. I. Mudawar and D. C. Wadsworth, Critical heat flux from a simulated chip to a confined rectangular impinging jet of dielectric liquid, *Int. J. Heat Mass Transfer* **34**(6), 1465–1479 (1991).
5. D. C. Wadsworth and I. Mudawar, Enhancement of single-phase heat transfer and critical heat flux from an ultra-high-flux simulated microelectronic heat source to a rectangular impinging jet of dielectric liquid, *ASME J. Heat Transfer* **114**(3), 764–768 (1992).
6. W. M. Rohsenow, A method of correlating heat transfer data for surface boiling liquids, *Trans. ASME* **74,** 969 (1952).
7. J. C. Chen, A correlation for boiling heat transfer to saturated fluids in convective boiling, *Int. Engng Chem. Process Des. Dev.* **5,** 322–335 (1966).
8. R. W. Lockhart and R. C. Martinelli, Proposed correlation of data for isothermal two-phase two-component flow in pipes, *Chem. Engng Process* **45,** 39–48 (1949).
9. C. T. Chang, Hydrodynamic and thermal field characteristics of two-phase jet impingement flows, Ph.D. Dissertation, Department of Mechanical Engineering, University of Wisconsin–Milwaukee (1992).